

DOI: 10.1002/cbic.200900669

## Protein Incorporation in Giant Lipid Vesicles under Physiological Conditions

Paige M. Shaklee,<sup>\*[a], [b]</sup> Stefan Semrau,<sup>[a]</sup> Maurits Malkus,<sup>[a]</sup> Stefan Kubick,<sup>[c]</sup> Marileen Dogterom,<sup>[b]</sup> and Thomas Schmidt<sup>[a]</sup>

One of the most essential components of a cell is the cell membrane. It forms both a protective boundary and a via for communication with the external environment. Because cell membranes are highly complex, simplified model systems in the form of giant vesicles (GVs) have been used extensively in vitro. GV are attractive membrane models because they can be produced easily with the electroformation method, their sizes are comparable to natural cell sizes ranging from tens to hundreds of micrometers in diameter, and the choice for the types of lipids that can be used is broad.<sup>[1]</sup> GV are not only used to study lipid heterogeneity<sup>[2–6]</sup> but also to examine the interaction of proteins with the membrane.<sup>[7–11]</sup> However, the incorporation of proteins in GV is difficult. Thus far only stable (small) membrane proteins have been successfully incorporated in GV in a functional form.<sup>[12]</sup> Compared to the gentle hydration method in which GV are formed by spontaneous swelling, the classic electroformation method yields larger vesicles, which also have fewer defects.<sup>[13]</sup> Despite its many advantages classic electroformation requires a low salt or saltless solution;<sup>[12, 14]</sup> this severely limits the choice of proteins that can be studied. Applications of this method that require salt solutions rely on buffer exchange after electroformation is completed.<sup>[15]</sup> Unfortunately, alternative methods to electroformation that can be applied in the presence of high salt solutions, such as spontaneous swelling or the freeze-thaw method,<sup>[16]</sup> are not optimally adapted for incorporation of proteins. Swelling methods typically require higher temperatures<sup>[17–19]</sup> that limit the lifetime of proteins in an experiment. Though freeze-thaw methods<sup>[16]</sup> are useful for making vesicles in salt buffers, it is widely known that proteins degrade with each subsequent freeze-thaw cycle, so that the method is not ideal for studies with sensitive proteins. Moreover, the inverse emulsion method<sup>[20]</sup> and microfluidic jetting<sup>[21]</sup> are also not suited for membrane proteins.

Here, we present two new applications of a specialized electroformation method, developed recently, that can produce GV under physiologically relevant salt conditions by applying

an electric field with a high frequency.<sup>[22, 23]</sup> 1) We create GV from native subcellular membranes containing transmembrane proteins. We produce, for the first time, GV containing transmembrane proteins that require post-translational modifications. 2) We load GV with biopolymer proteins as large as 110 kDa during electroformation at low temperatures, and show that the encapsulated proteins not only retain their function but also give shape to the GV.

First, we control the membrane composition of the GV using native membrane material. These native membranes are acquired from eukaryotic cells by a mild extraction procedure, which retains intact subcellular structures from the endoplasmic reticulum (ER). Membrane proteins are incorporated in these membranes by a novel in vitro transcription–translation procedure.<sup>[24–26]</sup> In this procedure, fully described in ref. [27], properly folded and biologically active membrane proteins are synthesized in vitro in cell extracts. This approach extends upon earlier methods by using prokaryotic expression systems,<sup>[28]</sup> which lack the ability to express proteins requiring post-translational modifications. Here, we incorporate a protein that requires such modification. Our in vitro translation reaction is comprised of the cell extract, purified mRNA encoding for the protein, complete amino acids, ATP and GTP. The mRNA codes for the membrane anchor of the small GTPase H-Ras (20–25 kDa), which contains the CAAX motif fused to eYFP (eYFP-CAAX).<sup>[29]</sup> The formation of the membrane anchor of H-Ras requires post-translational modification in the form of covalent attachment of fatty acids (palmitoylation).

By electroformation in saline buffer, GV containing eYFP-CAAX are formed. Figure 1 shows the cell extract on the surface of the electroformation chamber just prior to electroformation. Membrane material is colocalized with the cell extract

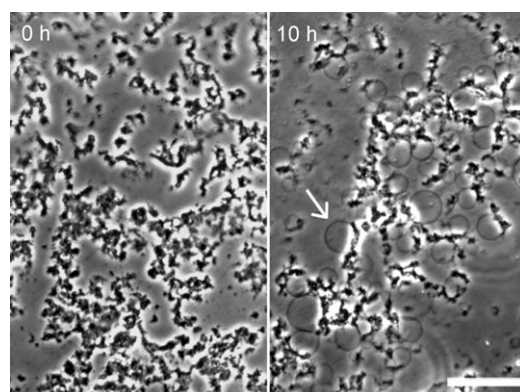


**Figure 1.** Electroformation of GV from cell extracts. Phase-contrast image of eukaryotic cell extract before electroformation (left) and after 10 h of electroformation (right). The white arrow points at a GV that has formed during electroformation; scale bar 50  $\mu$ m.

[a] Dr. P. M. Shaklee,<sup>\*</sup> Dr. S. Semrau,<sup>\*</sup> M. Malkus, Prof. Dr. T. Schmidt  
Physics of Life Processes, Leiden Institute of Physics  
Leiden University, Niels Bohrweg 2, 2333 CA, Leiden (The Netherlands)  
Fax: (+31) 71-527-5936  
E-mail: p.shaklee@amolf.nl

[b] Dr. P. M. Shaklee,<sup>\*</sup> Prof. Dr. M. Dogterom  
FOM Institute for Atomic and Molecular Physics (AMOLF)  
Science Park 104, 1098 XG, Amsterdam (The Netherlands)

[c] Dr. S. Kubick  
Fraunhofer Institute for Biomedical Engineering, IBMT  
Am Mühlenberg 13, 14476 Potsdam–Golm (Germany)

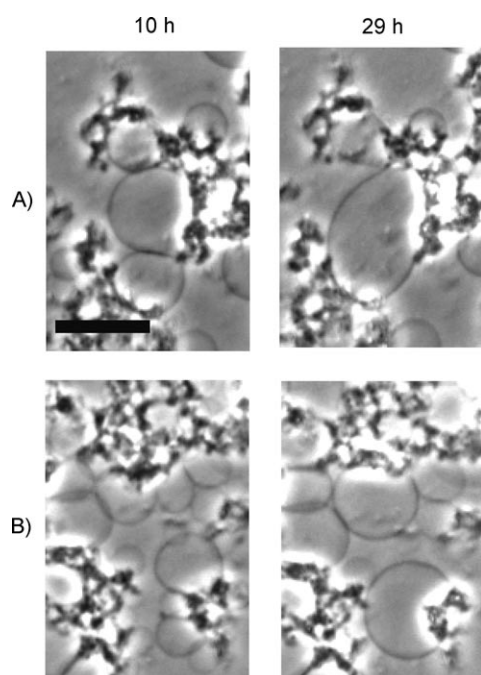
[\*] These authors contributed equally to this work.

Supporting information for this article is available on the WWW under <http://dx.doi.org/10.1002/cbic.200900669>.

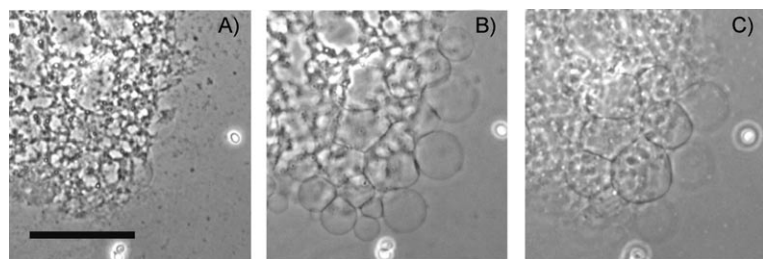
as verified by fluorescent membrane staining (data not shown). After  $\sim 5$  h,  $\mu\text{m}$  sized vesicles comprised of purely native membrane are visible and continue to grow by fusion (Figure 1). During electroformation GV's always stay attached to patches of cell extract showing that they form directly from the extract.

Figure 2 zooms in on the fusion process over an extended period of time. We find that the vesicles prepared in high salt have the same spatial size distribution as those formed by classical electroformation<sup>[30]</sup> (Figure 3).

Although GV's initially adhere to the cell extract, they can be harvested from the electroformation chamber and individually studied. Figure 4 shows a membrane-localized fluorescence signal on a GV, which shows that the membrane anchor is properly inserted into the membrane.



**Figure 2.** Vesicles fuse during electroformation. Phase-contrast images of vesicles after 10 and 29 h of electroformation. A) and B) Two different regions of the sample where the vesicles fuse; scale bar 25  $\mu\text{m}$ .



**Figure 3.** Layered size distribution of vesicles formed after 15 h electroformation. Phase-contrast images showing the same region of the electroformation chamber at different focal depths: A) directly on the glass, B) above the glass, and C) the top-most layer of vesicles. The vesicle size increases with depth, which is typical for electroformation,<sup>[30]</sup> scale bar 50  $\mu\text{m}$ .

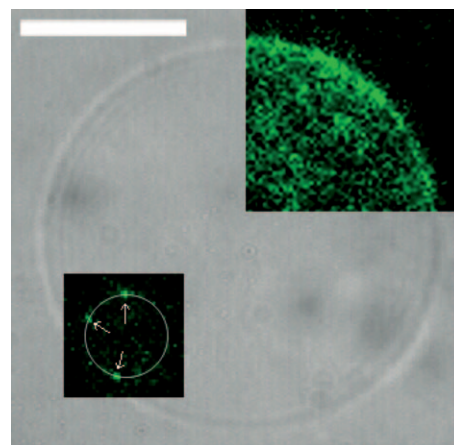


**Figure 4.** Membrane-localized eYFP. Wide-field image of a GV harvested from the electroformation chamber; scale bar 10  $\mu\text{m}$ . Top right inset: detail of fluorescence image of the same GV showing membrane localization of eYFP-CAAX. Lower left inset: fluorescence image of a GV (indicated by the white circle) with three single, mobile eYFP-CAAX molecules in the membrane (indicated by arrows); image  $9 \times 9 \mu\text{m}$ .

After sufficient bleaching we also observed individual mobile, diffraction limited eYFP signals (Figure 4, lower left inset). By fitting a two-dimensional Gaussian function to single diffraction limited spots (Figure 5B) we found the position of the signals with subdiffraction accuracy and the number of photons detected during the illumination time of 3 ms. Figure 5A shows a histogram of the number of detected photons coming from individual diffraction limited spots. From this measurement we determine an average emission intensity of  $\sim 950$  photons per ms for a single signal. This value is in good agreement with the intensity measured for single eYFP-CAAX in HEK cells.<sup>[31]</sup> These results suggest that the diffraction limited signals can be ascribed to single eYFP-CAAX molecules.

To further substantiate this conclusion we tracked the movement of the diffraction-limited spots. A typical trajectory is shown in Figure 5C. We analyze the positions of 829 eYFP signals with particle image correlation spectroscopy (PICS)<sup>[32]</sup> to determine the mean squared displacement (MSD; Figure 5D). Since we track the eYFP signals in optical sections around the equator of the vesicles (Figure 4, inset) over short time periods the observed movement of the molecules corresponds to one-dimensional diffusion. Consequently, we fit the measured MSD with a 1D diffusion model:  $\text{MSD}(\Delta t) = 2D\Delta t + 4\sigma^2$ . Where  $D$  is the diffusion coefficient,  $\Delta t$  the time lag between two consecutive images and  $\sigma$  the one-dimensional accuracy for the determination of the single molecule positions. The model fits the data with a diffusion coefficient of  $D = (0.07 \pm 0.01) \mu\text{m}^2\text{s}$  and a positional accuracy of  $\sigma = (125 \pm 30) \text{nm}$ . The measured value is smaller than the diffusion coefficient found for single eYFP-CAAX in the plasma membrane of cells ( $D \sim 0.4 \mu\text{m}^2\text{s}$ ).<sup>[29]</sup> This deviation might be explained by the fact that the GV's studied here are derived from the ER, which has a different membrane composition.

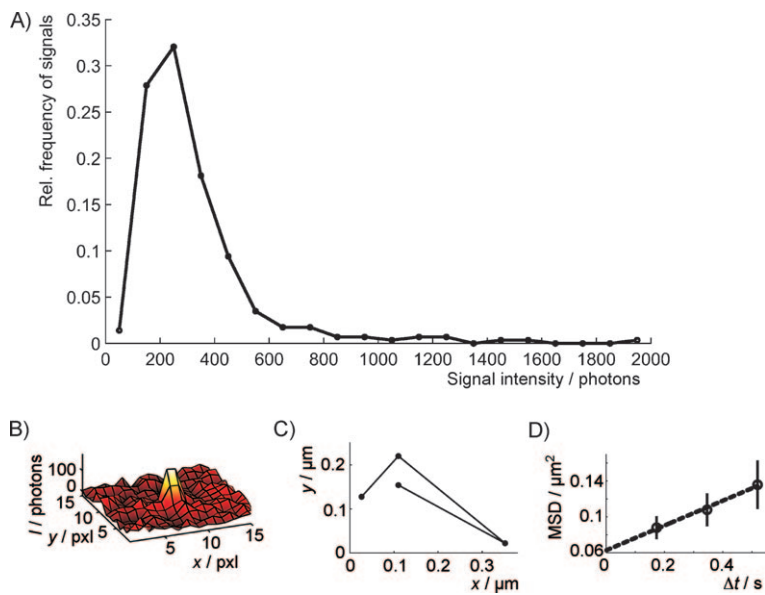


**Figure 5.** Characterization of eYFP signals. A) Histogram of the number of photons coming from single diffraction-limited spots during 3 ms of illumination with 514 nm light at an intensity of  $3 \text{ kW cm}^{-2}$ . The mean number of photons is  $\sim 340$ . The total detection efficiency of our apparatus is  $\eta = 0.12$  so that the average emission intensity is  $\sim 950$  photons per ms; bin size: 100 photons. B) A single diffraction limited eYFP signal. C) A typical trajectory of an eYFP signal. The time-lag between consecutive positions is 173 ms. D) Mean squared displacement (MSD) of eYFP signals. The positions of 829 eYFP signals were analyzed with particle image correlation spectroscopy<sup>[32]</sup> to determine the MSD. A model for 1D diffusion (----) fits the measured MSD with a diffusion coefficient of  $D = (0.07 \pm 0.01) \mu\text{m}^2 \text{ s}^{-1}$ .

Second, as a precursor to protein encapsulation in vesicles, we confirmed that GVs can be formed from synthetic lipids in high salt buffers<sup>[22,23]</sup> (Figure 6A); moreover, we show that  $1 \mu\text{m}$  sized beads are successfully enveloped by these GVs (Figure 6B).

Unlike beads, proteins are far more sensitive to local salt conditions and we verify that proteins that require high salt buffers can be encapsulated during electroformation. These proteins retain their function: eYFP is encapsulated and still fluoresces after electroformation (Figure 6C). We further show that protein assemblies still function after electroformation by exploiting the properties of self-assembling biopolymer proteins, namely, tubulin. First, tubulin proteins are incorporated into GVs during electroformation at low temperatures to suppress polymerization. Then the temperature is increased and tubulin successfully polymerizes to form

microtubules in the presence of GTP. The microtubules actively exert pushing forces from the inside of the GV, reshaping the GV (Figure 6D).<sup>[7,8]</sup> The tubulin/microtubules retain their property of “dynamic instability”, in which the microtubule switches between growing and shrinking phases as shown in radical, dynamic shape changes of the membrane protrusion in the time series and inset of Figure 6D. (The movie from which these images are taken is provided as Supporting Information.) The microtubules deform the GVs at speeds ranging from  $0.3$  to  $5.7 \mu\text{m min}^{-1}$ , which is in agreement with microtubule growth speeds reported by others.<sup>[33]</sup>

In order to determine the efficiency of protein encapsulation inside the vesicles, we examined the percentage of beads that are encapsulated. We consider beads as an extremum for encapsulation because the large ( $1 \mu\text{m}$ ) size of the beads suggests they will be much less efficiently encapsulated in GVs than smaller proteins (e.g., tubulin). We find that for a bead density of  $(0.02 \pm 0.01) \mu\text{m}^{-2}$ , and GV density of  $(0.01 \pm 0.01) \mu\text{m}^{-2}$ , an average of  $0.36 \pm 0.34$  GVs have one or more beads encapsulated.

We only consider GVs between 3 and  $15 \mu\text{m}$  in these statistics because intriguingly, GVs that are smaller than  $3 \mu\text{m}$  in diameter never have beads inside. The largest GVs in an electroformation chamber are the first to initially swell. The vesicles that begin to swell the first are likely from the uppermost lipid layer on the surface of the electroformation chamber because this layer is in most direct contact with the water in the

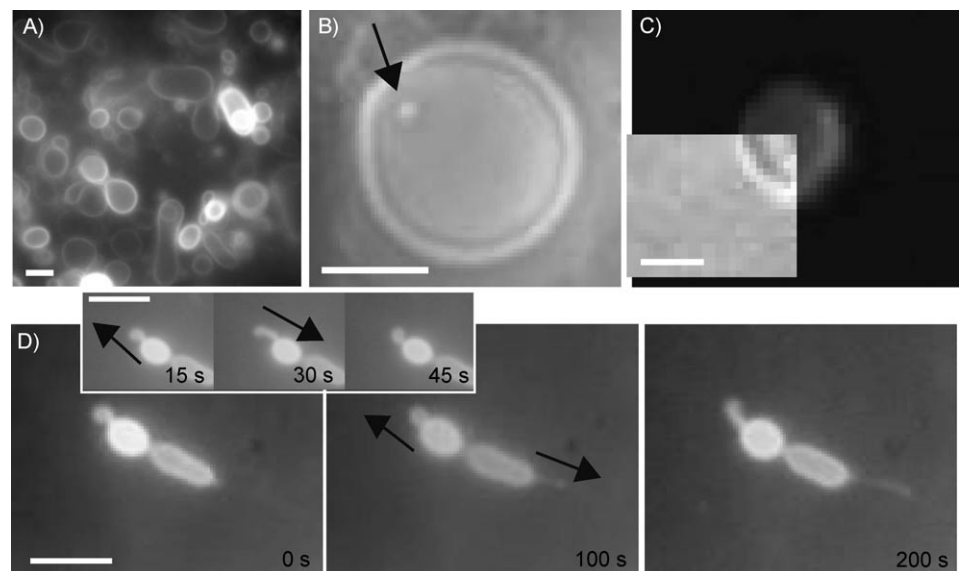


**Figure 6.** Proteins retain function inside GVs. A) GVs formed under physiological conditions (in MRB40). B) A  $1 \mu\text{m}$  polystyrene bead (indicated by the arrow) encapsulated by a GV. C) Fluorescence image of a GV containing eYFP incorporated during electroformation; the lower-left overlay is a phase-contrast image of the vesicle. D) Time series showing the dramatic shape changes of GVs deformed by dynamic GTP microtubules grown at  $37^\circ\text{C}$ . Microtubules deform the vesicle at speeds of up to  $5.7 \mu\text{m min}^{-1}$ . Inset shows growth followed by retraction of a membrane protrusion due to microtubule depolymerization; all scale bars are  $5 \mu\text{m}$ . (The movie from which these images are taken is provided as Supporting Information.)

chamber. We think the beads are most likely to be encapsulated in the initial GVs because the uppermost layer initially changes shape the most dramatically in response to water; this suggests an ease of access for the beads to slip beneath the swelling lipid bilayer. Because the concentration of tubulin protein used in our experiments is much higher than the concentration of beads and they are 100-times smaller than the beads, we do not expect the concentration of proteins outside the GVs to strongly differ from the concentration of proteins inside the GVs.

To summarize, we have shown two ways to incorporate proteins into GVs with electroformation in high salt solutions. We are able to tailor the protein content of the membrane using membrane material from eukaryotic cell extracts. We can also encapsulate proteins inside GVs and show that these proteins remain functional. Microtubules that are encapsulated retain their dynamic properties as evidenced by active deformation of the GV shape. As an outlook, our method also opens doors to investigating membrane properties of native, intracellular membranes. The cell extracts used in this study contain membrane from the ER<sup>[27]</sup> so that the influence of ER on membrane parameters, such as the bending rigidity, can be studied in extract-derived GVs. Finally, our method could be used to study signal transduction cascades with several membrane proteins in a controlled environment.

## Experimental Section

### Membrane proteins incorporated in GVs by electroformation:

Fall army worm (*Spodoptera frugiperda*, *Sf*) cells were grown in well-controlled fermenters at 27 °C in an animal component free insect cell medium. During a period of exponential growth, at a density of approximately  $4 \times 10^6$  cells mL<sup>-1</sup>, *Sf* cells were collected by centrifugation and washed with a HEPES-based homogenization buffer consisting of HEPES-KOH (40 mM, pH 7.5), KOAc (100 mM) and DTT (4 mM). Finally, the *Sf* cell pellet was resuspended in an appropriate volume of homogenization buffer to achieve a cell density of approximately  $2 \times 10^8$  cells mL<sup>-1</sup>. Resuspended *Sf* cells were lysed mechanically and the homogenate was centrifuged at 10 000 *g* for 10 min at 4 °C to remove nuclei and debris. The resulting supernatant was applied to a Sephadex G-25 column and fractions with the highest RNA/protein concentrations were pooled. Aliquots of the *Sf* lysate were immediately frozen in liquid nitrogen and then stored at -80 °C to preserve maximum activity. This mild treatment yields final extracts that retain intact subcellular membranous structures derived from the ER. Linked transcription–translation was performed in the high-yield mode: an aliquot from the initial transcription step was purified by an intermediate gel filtration step (DyeEx spin columns, Qiagen) to clean the mRNA prior to addition to the cell-free extract. In vitro translation reaction mixes were composed of 25% (*v/v*) lysate, mRNA encoding the membrane anchor of H-Ras, which contains the CAAX motif, fused to eYFP (eYFP-CAAX),<sup>[29]</sup> complete amino acids (200 μM), ATP (1.75 mM) and GTP (0.45 mM). The insect cell extract based in vitro translation system is now commercially available (EasyXpress insect kit 1 II, Qiagen). Translational activity and localization of the synthesized protein was determined by fluorescence microscopy after the incubation time of 90 min at 27 °C. Cell-free protein synthesis was performed at RiNA GmbH (<http://www.rina-gmbh.de/>).

The extract-derived reaction mix (5 μL) was applied to a surface of ~50 mm<sup>2</sup> on an indium tin oxide (ITO)-coated glass slide and dried under a continuous flow of nitrogen. This drying step was necessary to bring the extract, which does not sediment otherwise, in close contact with the ITO glass for successful electroformation. The resulting layer had a thickness of a few hundred nanometers as inferred from visible colored interference fringes when viewed in reflection. Thicknesses larger or much smaller than this did not result in vesicle formation. The procedure yielded functional (i.e., fluorescent) proteins, implying that the “partial” drying step does not denature the protein. Immediately after being dried PBS (~60 μL, without magnesium and calcium) was added and the electroformation chamber was completed by a polydimethylsiloxane (PDMS) spacer with a thickness of ~1.25 mm and a second ITO coated slide to yield a final chamber volume of 70 μL. In contrast to the original electroformation method,<sup>[1]</sup> we applied an AC electric field at a higher frequency<sup>[23]</sup> as follows: an AC electric field (~6000 Vm<sup>-1</sup>, 500 Hz) was applied for up to 30 h at 20 °C<sup>[22,23]</sup> to form GVs (Figure 1). The successful insertion of the membrane anchor of the eYFP-CAAX construct into the membrane was verified by observing a membrane-localized fluorescence signal (Figure 4).

**Encapsulation of proteins during electroformation:** 1,2-Dioleoyl-*sn*-glycero-3-phosphocoline (DOPC), 1,2-dioleoyl-*sn*-glycero-3-phosphoethanolamine-*N*-(cap biotinyl) (DOPE-Bio), and 1,2-dioleoyl-*sn*-glycero-3-phosphoethanolamine-*N*-(lissamine rhodamine B sulfonyl) (DOPE-Rh) were purchased from Avanti Polar Lipids. Tubulin and GTP were purchased from Cytoskeleton, Inc. (Denver, CO, USA). The eYFP was purified from *E. coli* SG13009 with the inserted plasmid pMP6088 clone 6244 (Qiagen).<sup>[31]</sup> Lipids were resuspended in chloroform, and DOPE-Rh (0.2 mol%) was added to DOPC to a final concentration of 5 mg mL<sup>-1</sup>. The lipid solution (1 μL) was dropped onto one of two ITO-coated coverslips purchased from Diamond Coatings, Ltd. (Cradley Heath, West Midlands, UK). The lipids were distributed on the glass by the “rock-and-roll” method<sup>[1]</sup> and dried for 30 min under continuous nitrogen flow. An 8 μL volume chamber was constructed from the two glass plates, the dried lipids on the bottom glass, and a PDMS spacer. The chamber was filled with a solution of eYFP (20 μM) or tubulin (38 μM) in MRB40 (40 mM PIPES, 4 mM MgCl<sub>2</sub>, 1 mM EGTA, pH 6.8, 100 mOsm) and GTP (4 mM, conditions for spontaneous nucleation) and/or polystyrene beads, and placed at 4 °C. An AC electric field was applied at 500 Hz with a linear voltage increase from 50 to 1300 Vm<sup>-1</sup> over 30 min, held at 1300 Vm<sup>-1</sup> for 90 min, then the frequency was decreased linearly from 500 to 50 Hz over 30 min. During imaging GV samples with GTP microtubules were heated to 37 °C by using a heating foil mounted on top of the sample chamber.

**Imaging:** Images were acquired on an epifluorescence inverted microscope equipped with a CCD camera (Axiovert 40CFL, Carl Zeiss, Inc.; WAT-902H ULTIMATE, Watec, Japan). The image in the inset in Figure 4 was acquired on a wide-field microscope optimized for single molecule fluorescence imaging.<sup>[29]</sup>

## Acknowledgements

The authors thank Dr. Sylvie Olthuis-Meunier for purification of eYFP and Dr. Kramer Campen for critical reading of the manuscript. This work is part of the research program of the “Stichting voor Fundamenteel Onderzoek der Materie (FOM)”, which is financially supported by the Nederlandse Organisatie voor Wet-

schappelijk Onderzoek (NWO) within the program on Material Properties of Biological Assemblies (grants FOM-L1708M and FOM-L1707M).

**Keywords:** biomimetics · electroformation · membranes · protein incorporation · single molecule tracking

- [1] M. I. Angelova, S. Soleau, P. Meleard, J. F. Faucon, P. Bothorel, *Prog. Colloid Polym. Sci.* **1992**, *89*, 127–131.
- [2] C. Dietrich, L. A. Bagatolli, Z. N. Volovyk, N. L. Thompson, M. Levi, K. Jacobson, E. Gratton, *Biophys. J.* **2001**, *80*, 1417–1428.
- [3] T. Baumgart, S. T. Hess, W. W. Webb, *Nature* **2003**, *425*, 821–824.
- [4] N. Kahya, D. Scherfeld, K. Bacia, B. Poolman, P. Schwille, *J. Biol. Chem.* **2003**, *278*, 28109–28115.
- [5] S. L. Veatch, S. L. Keller, *Phys. Rev. Lett.* **2005**, *94*, 148101.
- [6] S. Semrau, T. Idema, L. Holtzer, T. Schmidt, C. Storm, *Phys. Rev. Lett.* **2008**, *100*, 088101.
- [7] D. K. Fygenson, J. F. Marcko, A. Libchaber, *Phys. Rev. Lett.* **1997**, *79*, 4497–4500.
- [8] T. Kaneko, T. J. Itoh, H. Hotani, *J. Mol. Biol.* **1998**, *284*, 1671–1681.
- [9] F. Nomura, M. Honda, S. Takeda, T. Inabe, K. Takiguchi, T. J. Itoh, A. Ishijima, T. Umeda, H. Hotani, *J. Biol. Phys.* **2002**, *28*, 225–235.
- [10] C. Leduc, O. Campàs, K. B. Zeldovich, A. Roux, P. Jolimaitre, L. Bourel-Bonnet, B. Goud, J.-F. Joanny, P. Bassereau, J. Prost, *Proc. Natl. Acad. Sci. USA* **2004**, *101*, 17096–17101.
- [11] P. M. Shaklee, T. Idema, G. Koster, C. Storm, T. Schmidt, M. Dogterom, *Proc. Natl. Acad. Sci. USA* **2008**, *105*, 7993–7997.
- [12] M. K. Doeven, J. H. A. Folgering, V. Kraskinov, E. R. Geertsma, G. van den Bogaart, B. Poolman, *Biophys. J.* **2005**, *88*, 1134–1142.
- [13] N. Rodriguez, F. Pincet, S. Cribier, *Colloids Surf. B* **2005**, *42*, 125–130.
- [14] D. Merkle, N. Kahya, P. Schwille, *ChemBioChem* **2008**, *9*, 2673–2681.
- [15] D. J. Estes, M. Mayer, *Biochim. Biophys. Acta* **2005**, *1712*, 152–160.
- [16] D. D. Lasic, *Biochem. J.* **1988**, *256*, 1–11.
- [17] K. Akashi, H. Miyata, H. Itoh, K. Kinoshita, Jr., *Biophys. J.* **1998**, *74*, 2973–2982.
- [18] Y. Yamashita, M. Okaa, T. Tanakab, M. Yamazaki, *Biochim. Biophys. Acta* **2002**, *1561*, 129–134.
- [19] Y. Tamba, S. Ohba, M. Kubota, H. Yoshioka, H. Yoshioka, M. Yamazaki, *Biophys. J.* **2007**, *92*, 3178–3194.
- [20] S. Pautot, B. J. Frisken, D. A. Weitz, *Langmuir* **2003**, *19*, 2870–2879.
- [21] J. C. Stachowiak, D. L. Richmond, T. H. Li, A. P. Liu, S. P. Parekh, D. A. Fletcher, *Proc. Natl. Acad. Sci. USA* **2008**, *105*, 4697–4702.
- [22] T. Pott, H. Bouvrais, P. Meleard, *Chem. Phys. Lipids* **2008**, *154*, 115–119.
- [23] L.-R. Montes, A. Alonso, F. M. Goni, L. A. Bagatolli, *Biophys. J.* **2007**, *93*, 3548–3554.
- [24] S. Kubick, J. Schacherl, H. Fleischer-Notter, E. Royall, L. O. Roberts, W. Stiege in *Cell-Free Protein Synthesis* (Ed.: J. R. Swatz), Wiley-VCH, Weinheim, **2003**, pp. 209–217.
- [25] S. Kubick, H. Merk, W. Stiege, U. von Groll, J. Drees, F. Schäfer, *Qiagen News* **2005**, *2*, 41–43.
- [26] U. von Groll, S. Kubick, H. Merk, W. Stiege, F. Schäfer in *Cell-Free Expression* (Eds.: T. Kudlicki, F. Katzen, R. Bennett), Landes Bioscience, **2007**.
- [27] S. Kubick, M. Gerrits, H. Merk, W. Stiege, V. A. Erdmann in *Current Topics in Membranes*, Vol. 63, Elsevier, **2009**, Chapter 2.
- [28] S. M. Nomura, K. Tsumoto, T. Hamada, K. Akiyoshi, Y. Nakatani, K. Yoshikawa, *ChemBioChem* **2003**, *4*, 1172–1175.
- [29] P. H. M. Lommerse, G. A. Blab, L. Cognet, G. S. Harms, B. E. Snaar-Jagalska, H. P. Spaink, T. Schmidt, *Biophys. J.* **2004**, *86*, 609–616.
- [30] L. Mathivet, S. Cribier, P. F. Devaux, *Biophys. J.* **1996**, *70*, 1112–1121.
- [31] G. S. Harms, L. Cognet, P. H. M. Lommerse, G. A. Blab, T. Schmidt, *Biophys. J.* **2001**, *80*, 2396–2408.
- [32] S. Semrau, T. Schmidt, *Biophys. J.* **2007**, *92*, 613–621.
- [33] D. K. Fygenson, E. Braun, A. Libchaber, *Phys. Rev. E* **1994**, *50*, 1579–1588.

Received: November 4, 2009

Published online on December 10, 2009